ON PHASE TRANSFORMATIONS IN AGGLOMERATED FLUX OF SALT-OXIDE SLAG SYSTEM AT HEATING

V.E. SOKOLSKY[1], **A.S. ROIK**[1], **A.O. DAVIDENKO**[1], **V.I. GALINICH**[2], **I.A. GONCHAROV**[2],
D.D. MISHCHENKO[2] and **V.S. TOKAREV**[2]
[1]Taras Shevchenko National University, Kiev, Ukraine
[2]E.O. Paton Electric Welding Institute, NASU, Kiev, Ukraine

Electron-optical and X-ray diffraction methods were used to study the structure and phase composition of agglomerated welding flux of SiO_2–Al_2O_3–CaF_2–MgO system.

Keywords: *arc welding, agglomerated welding flux, electron-optical and X-ray examination methods, interaction reactions, phase transformations*

Agglomerated flux production requires much less power consumption than fused flux manufacture. Ceramic fluxes are made by mixing charge components with binder (liquid glass) in the pelletizer with subsequent baking at the temperature of 600–700 °C [1, 2]. After long-term isothermal soaking in the molten state at 1500–1750 °C, that is higher than the flux melting temperature by 300–600 °C, fused flux is quenched by «wet granulation» (pouring a melt jet into water). Therefore, it has a structure close to that of the melt. Agglomerated flux mainly preserves the crystalline structure of the initial charge materials. The fast process of welding with agglomerated fluxes in the presence of various temperature zones in the weld pool cannot completely ensure formation of slag with preferable structures of liquid type [3], whereas description of the processes of structure formation in them is practically absent in scientific publications. Thus, integrated structural studies of agglomerated fluxes are of considerable scientific interest.

Experimental conditions. Powder-like sample of flux on graphite substrate was subjected to electron-optical examination in raster electron microscope JSM-7700F with an attachment for X-ray spectral analysis. A massive slag sample that was removed from the crucible after complete melting of the flux (1500 °C) was studied separately from the side of the bottom and the surface. To prevent the influence of charging by the electron beam in the entire low-conducting flux, a layer of pure platinum of 3 nm thickness was spray-deposited on the sample surface. X-ray analysis (CuK_α-radiation, DRON-3M diffractometer) was conducted after granulation and drying of the flux, as well as complete melting from the side of the crucible bottom and surface.

High-temperature X-ray investigations were conducted using high-temperature diffractometer, designed to study melts (MoK_α-radiation). Radiation monochromatization was performed with a couple of balanced differential Zr–Y filters [3]. Filming was conducted at temperatures of 600, 800, 1000, 1200, 1350 and 1450 °C in a high-temperature vacuum chamber in highly pure helium atmosphere.

Data of X-ray analysis were interpreted using Powdercell, Mercury structural programs, Match and Retrive data bases that are freely disseminated through the Internet. When studying the slag melt, calculations were performed using proprietary software [3].

Room temperature studies. Calculated relationship of the main components of MgO, Al_2O_3, SiO_2 and CaF_2 is given in Table 1. In the pelletizer sodium-potassium liquid glass was added to the crushed mechanical mixture of the main components. Baking at 500 °C was conducted after granulation and soaking in air. Composition of the obtained flux was determined using X-ray fluorescent analysis.

Data of X-ray phase analysis (Figure 1) show that after granulation and baking the sample contains only initial components — α-SiO_2, trigonal Al_2O_3, cubic MgO and CaF_2. X-ray phase analysis methods did not reveal any products of flux component interaction.

Table 2 gives micrographs and data of microanalysis of the sample bottom and surface after remelting in a molybdenum crucible. Micrographs of the crucible surface and bottom differ somewhat. From the bottom side the formed crystalline phases are more finely dispersed, voids are observed, in which gas bubbles accumulated, and cracks are clearly visible. The sample is not homogeneous. There is markedly less fluorine on the surface (0.99–3.50 at.%), whereas from the crucible bottom side (if we ignore the reduced amount of fluorine in the voids — reflection 1, spectrum 2), fluorine content is higher than 7 at.%. Light-coloured inclusions of the type of spectrum 3 in reflection 2 are also observed, where fluorine concentrations are considerable, although visually the area of these particles is small.

Note that the approximate ratio of components Ca:Al:Si = 1:2:2 (see Table 2) in most of the reflections corresponds to anorthite — lime felspar $Ca(Al_2Si_2O_8)$. Sodium content in these samples is

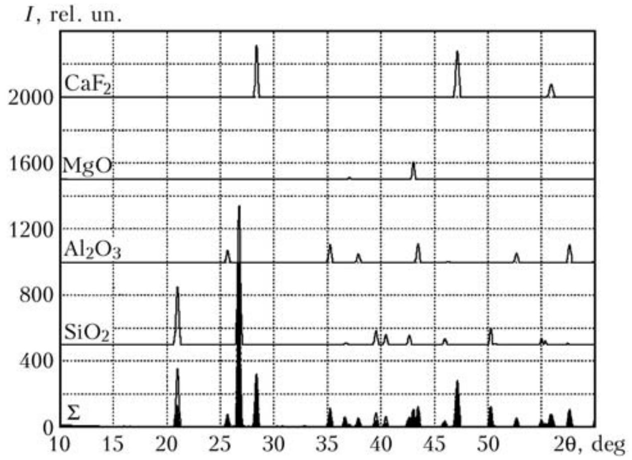

Figure 1. Roentgenograms of components of crushed to powder agglomerated flux and summation curve after improvement of profile based on SiO_2, Al_2O_3, MgO and CaF_2 elementary cells by Powdercell

much smaller than in samples before remelting. This means that alkali oxide is uniformly distributed across the volume after melting, rather than concentrating on particle surface as in the freshly prepared flux. From the bottom side fluorine content C_F is in the range of 3–16 at.%, whereas from the surface side C_F does not exceed 3.5 at.%. Fluorine content does not correlate with calcium content C_{Ca}, where $C_{Ca}/C_F \neq \neq 1:2$. Magnesium content is much higher from the bottom side than from the surface side (Figure 2). Also found here is the dependence of C_F in all the samples (both from the substrate side, and from the bottom side) on $C_{Ca + Mg}$, C_{Mg} and C_{Ca}. In our opinion, such a dependence of $C_{Ca + Mg}$ with the largest of the three correlation coefficients, is indicative of the fact that fluorine is partially redistributed between calcium and magnesium that suggests formation of calcium oxide at the expense of magnesium oxide.

Table 1. Composition of flux for surfacing, wt.%

Assessment	MgO	Al_2O_3	SiO_2	CaF_2	Na_2O	K_2O	Fe_2O_3
Calculated	10.0	25.0	40.0	25.0	–	–	–
Actual	8.9	22.6	42.0	22.9	1.4	0.8	1.4

X-ray phase analysis of a sample remelted at 1500 °C (Figure 3) shows that the main phases both from the substrate side and from the crucible bottom side are the triclinic (a =0.8192 nm, b = 1.2869 nm, c = 1.4180 nm, α = 93.18°, β = 115.63°, γ = 91.08°) and monoclinic (a = 0.8235 nm, b = 0.8630 nm, c = = 0.4833 nm, α = 90°, β = 89.37°, γ = 90°) modifications of anorthite. From the bottom side MgF_2 is present is small amounts (see Figure 3). Thus, X-ray phase analysis confirms the fact that at remelting calcium and magnesium exchange anions and in anorthite calcium is present (at least partially) in the oxide form and magnesium, partially, forms fluoride.

High temperature X-ray studies in the solid state. In order to trace the sequence of the reactions in the solid phase, ceramic flux crushed into powder was placed into a molybdenum crucible, which was located on the work table of high-temperature vacuum chamber of the diffractometer for melt investigation [3], and was subjected to high-temperature X-ray phase analysis. As shown by analysis, structural changes in

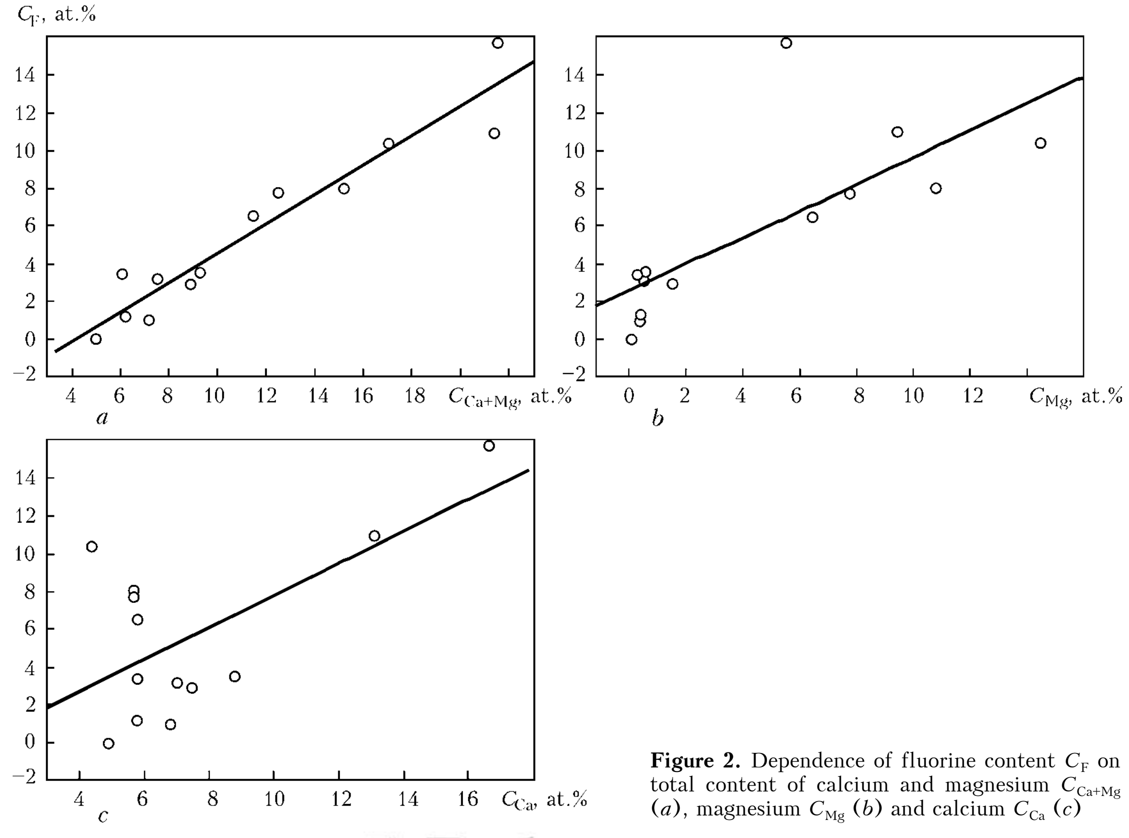

Figure 2. Dependence of fluorine content C_F on total content of calcium and magnesium C_{Ca+Mg} (a), magnesium C_{Mg} (b) and calcium C_{Ca} (c)

Table 2. Data of X-ray spectral (at.%) and visual analysis of remelted flux

Bottom, reflection 1					
Chemical element	Spectrum				
	1	2	3	4	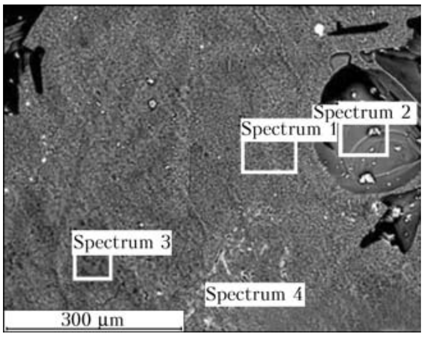
O	58.9	67.6	56.3	54.0	
F	8.0	3.4	10.3	10.9	
Na	0.2	0.3	0.4	0	
Mg	9.5	0.3	12.7	8.3	
Al	6.7	12.0	5.8	2.3	
Si	11.0	11.1	10.1	11.4	
Ca	5.7	5.8	4.4	13.1	
Ti	–	–	<0.1	–	

Bottom, reflection 2					
Chemical element	Spectrum				
	1	2	3	4	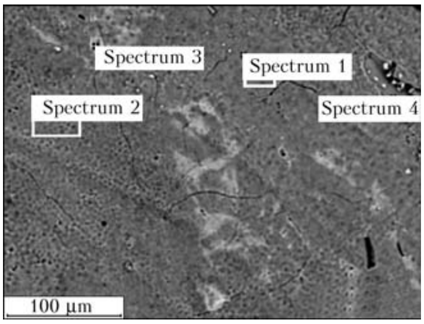
O	59.7	60.92	51.55	63.29	
F	7.7	6.48	15.63	3.17	
Na	0.1	0.14	0	0.02	
Mg	6.8	5.69	4.89	0.49	
Al	8.8	9.48	1.22	13.25	
Si	11.1	11.47	10.08	12.74	
Ca	5.7	5.81	16.64	7.04	

Surface, reflection 1				
Chemical element	Spectrum			
	1	2	3	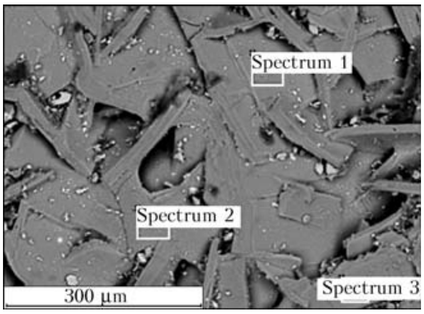
O	62.6	66.0	60.9	
F	2.9	1.0	3.5	
Na	0.1	0.3	0.3	
Mg	1.4	0.4	0.5	
Al	12.8	12.8	13.5	
Si	12.7	12.6	12.6	
Ca	7.5	6.8	8.8	

Surface, reflection 2			
Chemical element	Spectrum		
	1	2	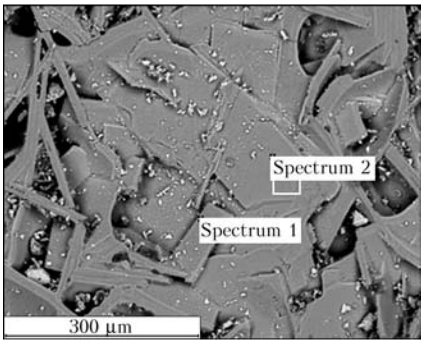
O	72.1	67.9	
F	–	1.2	
Na	0.1	0.1	
Mg	0.1	0.4	
Al	11.7	12.5	
Si	11.1	12.1	
Ca	4.9	5.8	

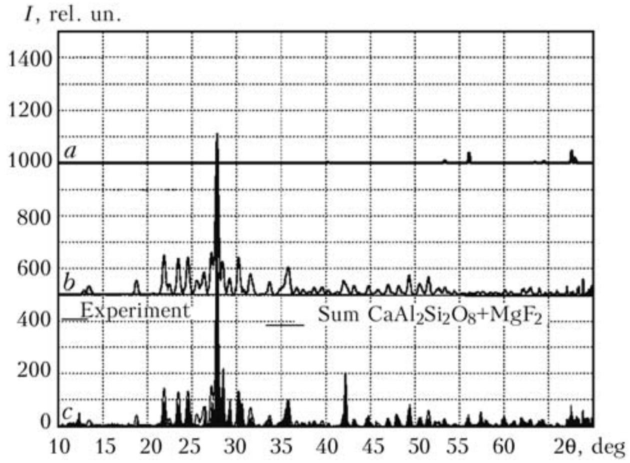

Figure 3. Diffraction patterns of flux at 1500 °C from the bottom side: *a*, *b* — improved profile of magnesium fluoride and anorthite, respectively; *c* — experiment and summary curve for monoclinal anorthite and magnesium fluoride (line with shaded area under the curve)

the sample occur in the entire temperature range (Figure 4). Up to 1200 °C these changes occur in the solid phase. At low temperatures transformations proceed slowly, and mainly run inside the phases. For instance, already at 600 °C, the most intensive peak responsible for 100 % intensity of hexagonal α-quartz decreases abruptly. At the same time, peaks appear which may be referred to other silicon modifications.

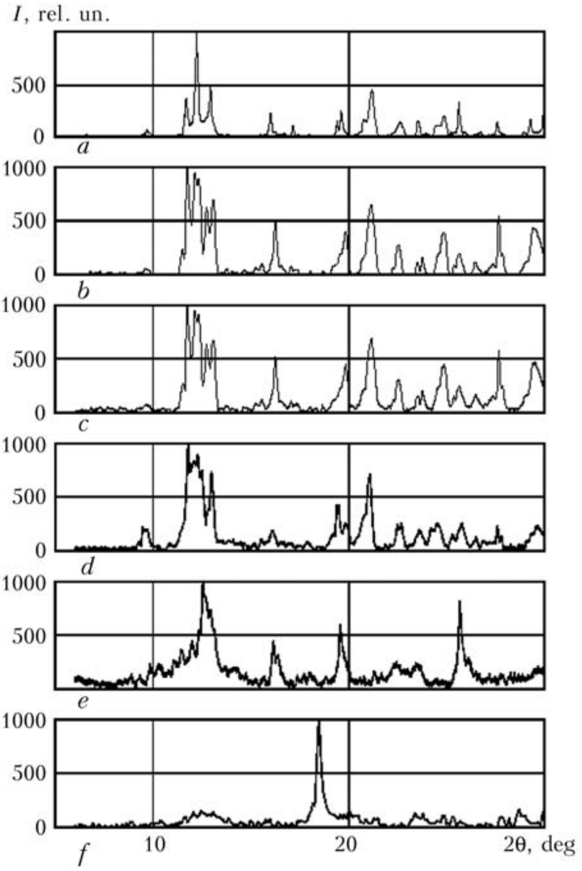

Figure 4. Diffraction patterns of flux at different temperatures: *a* — room temperature; *b*–*f* — 600, 800, 1000, 1200, 1200, 1350 °C, respectively

Interphase interactions start at higher temperatures. It should be taken into account that in an agglomerated flux the main components are inside the matrix from binder material (product of liquid glass heat treatment). Therefore, interphase interaction will occur as a result of diffusion of flux component atoms into the matrix, and vice versa. According to Sen's rule [4], diffusion rate is higher in the direction of the body with greater interatomic distances. Of all the flux components the largest interatomic distances ($R_{\text{cation–anion}}$) are realized in liquid glass manufacture from sodium-potassium silicate lump ($R_{\text{Na–O}}$ and $R_{\text{K–O}}$ distances), in connection with which liquid-glass based products are saturated by other flux components. Diffusion rate can be further increased as a result of vacancy formation at water evaporation from liquid glass (OH^- evaporating group and anion F^- replacing it, have close ionic radiuses of 0.118 and 0.115 nm, respectively).

Difficulties of interpretation of diffraction patterns of multicomponent materials, most of which have low symmetry, should be mentioned. For instance in Figure 5 one can see that MgF_2 reflections are overlapped by reflections of widened anorthite.

Interpretation of the obtained results should be performed using complex constitutional diagram of $Na_2O–Al_2O_3–MgO–CaO–SiO_2–CaF_2–MgF_2$, but such oxide-fluoride diagram is non-existent in scientific publications. The closest studied constitutional diagram is that of four-component $CaO–MgO–Al_2O_3–SiO_2$ system [4, 5], in which the field of anorthite solidification appears in the section of 15 % Al_2O_3 and ousts the fields of solidification of wollastonite ($Ca–SiO_2$) and piroxene ($MgSiO_3$). At 20 % Al_2O_3 the field of wollastonite solidification is absent, and that of piroxene is greatly narrowed. The section of 10 % MgO no longer has the field of calcium aluminate solidification, but has the fields of solidification of periclase (MgO), spinel (Al_2MgO), and cordierite ($Mg_2Al_4Si_5O_{18}$) [4]. It is characteristic that in the constitutional diagram of $CaO–MgO–Al_2O_3–SiO_2$

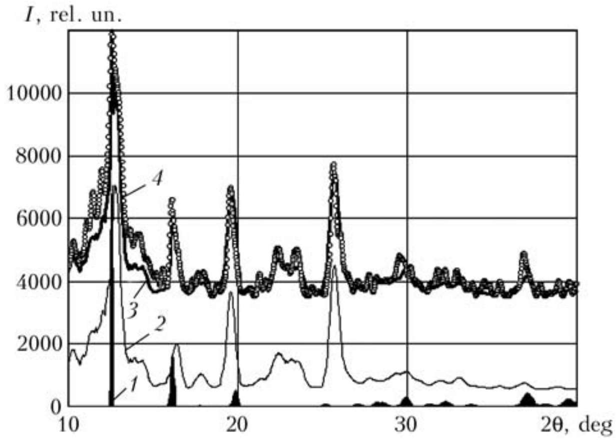

Figure 5. X-ray patterns of MgF_2 (*1*) and $Ca(Al_2Si_2O_8)$ with widened peak half-width after improvement of diffraction profile (*2*) by Powercell, total *1* + *2* (*3*) and experimental curve at 1200 °C (*4*)

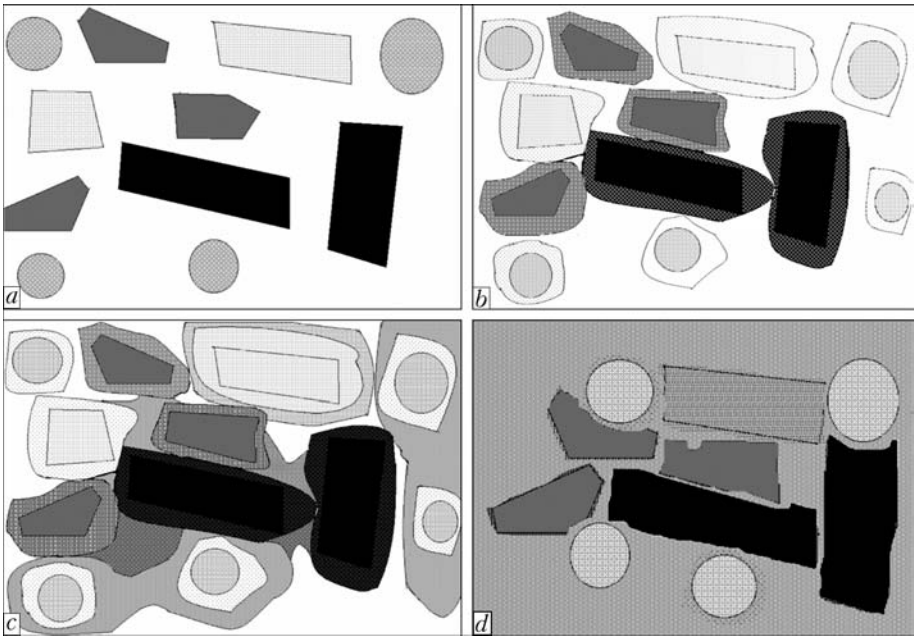

Figure 6. Structural changes at flux heating: *a*–*d* — first–fourth periods, respectively

system anorthite forms at small content of MgO (10–15 %), whereas spinels form at higher magnesium oxide contents.

Let us consider the mechanism of anion redistribution between calcium and magnesium cations. Let us give a simplified demonstration of chemical interaction in a mixture of solid reagents in binder material matrix (Figure 6). In the first stage components after granulation are placed into a binder matrix (Figure 6, *a*). At temperature rise diffusion on the phase contact surface increases considerably and surface layers saturated with contacting phases form in the binder matrix, based on products of liquid glass baking (Figure 6, *b*). In the third stage of the process more complex chemical compounds form that are based on interaction of boundary layers around the component inside the binding matrix (Figure 6, *c*). Further increase of temperature and component dissolution may lead to melting (probably, partial) and formation at first of local molten inclusions. Rate of substance diffusion between the molten groupings rises considerably. Diffusion between the solid and liquid components rises less significantly. Thus, at the final stage (Figure 6, *d*) a uniform liquid matrix and partially dissolved flux components form. If the silicate module of liquid glass is low, than dissolution of silicon in it with increase of silicate module may greatly lower the temperature of formation of the liquid sodium-silicate phase to 790 °C (lowest melting eutectics in Na_2O–SiO_2 has the composition of $Na_2O \cdot 2SiO_2 + SiO_2 +$ liquid, $T_m = 793$ °C). It is obvious that dissolution of other flux components lowers the temperature of sodium silicate. At further temperature rise, all the components either melt, or dissolve completely in the liquid phase with formation of a uniform homogeneous liquid phase.

At low baking temperatures (3rd period), more complex oxifluoride compounds, probably, form based on the products of decomposition of liquid glass and adjacent to it layer of several components (for instance, $AlCa_2Mg_5NaSi_7O_{22}F_2$). Such compounds cannot be stable in a broad temperature range, as they consist of a wide range of cations and anions with different charges and significant differences in ionic radii dimensions. Compounds of this type possibly do not have a completely formed crystalline structure or even exist in an amorphous form, as the time of their soaking at high temperatures is low (none of them were found in the roentgenograms, either). However, if they formed and then decomposed at high temperatures, then the possible decomposition of $AlCa_2Mg_5Si_7O_{22}F_2$ can be presented by one of the following equations:

$$2AlCa_2Mg_5NaSi_7O_{22}F_2 \rightarrow CaAl_2Si_2O_8 + MgF_2 + 3CaMg_3Si_4O_{12} + 2NaF, \quad (1)$$

$$2AlCa_2Mg_5NaSi_7O_{22}F_2 \rightarrow CaAl_2Si_2O_8 + 2MgF_2 + Ca_3Mg_8Si_{12}O_{35} + Na_2O, \quad (2)$$

$$2AlCa_2Mg_5NaSi_7O_{22}F_2 \rightarrow CaAl_2Si_2O_8 + MgF_2 + 3CaO + 9MgO + 12SiO_2 + 2NaF, \quad (3)$$

$$2AlCa_2Mg_5NaSi_7O_{22}F_2 \rightarrow CaAl_2Si_2O_8 + MgF_2 + 3CaO + 8MgO + 12SiO_2 + Na_2O, \quad (4)$$

proceeding from which formation of MgF_2 and anorthite should be anticipated. Such an assumption can be further confirmed by the fact that analysis of compounds of $AlCa_2Mg_5NaSi_7O_{22}F_2$ type in diffraction databases showed that all the complex oxyfluorides of this type have spatial group C 2/*m* and fluorine anions in them select magnesium cations as their closest neighbours, whereas calcium is surrounded by oxygen.

Thermal decomposition of such a compound into simpler components by one of the above formulas may lead to transformation of oxide-fluoride components

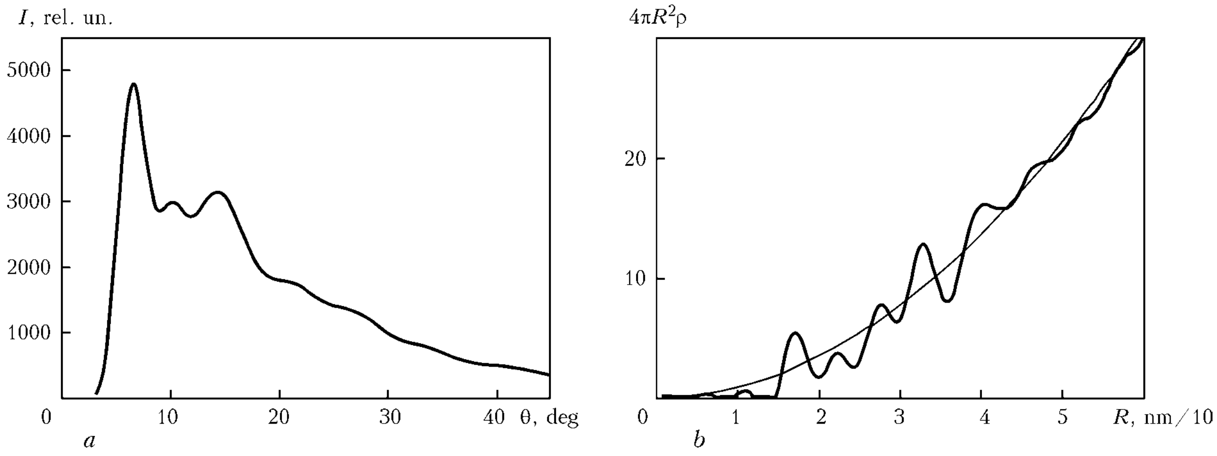

Figure 7. Curve of intensity of scattered X-rays from molten sample at 1450 °C (*a*), and curve of radial distribution of atoms (*b*)

with formation of MgF_2, CaO and anorthite. Formation of magnesium fluoride and anorthite by other mechanisms is also possible. Anorthite as fluorspar is one of the most widely spread minerals of the Earth's crust, it is identified in meteoritic material, deep material of the crust, and, possibly, in the mantle, that is indicative of its sufficient stability. Therefore, anorthite nuclei formed by one of reactions (1)–(4) can be incremented at the expense of other flux components of Al_2O_3 and SiO_2, as well as CaO_2 that formed by reaction (3), (4).

At 1200 °C the sample partially melts, and the crystalline phase also partially remains. At interaction of the liquid and solid phases there is a great increase both in the interaction surface (10^4–10^7) and intensity of mass transfer as a result of diffusion by several orders of magnitude [4]. Thus, the main components can dissolve in the liquid phase, with just crystalline anorthite (T_m = 1540 °C) and MgF_2 (T_m = 1261 °C) remaining.

At 1350 °C the diffraction pattern (see Figure 4) is unstable. In the first filming MgO reflections are present against the background of the liquid phase. One of the more complex compounds, probably, decomposed, part of which dissolved in the liquid phase. In the second and third filming MgO reflections disappear. However, crystalline peaks, which could not be identified, are present against the background of the liquid component.

X-ray examination of molten flux. Liquid phase forms completely at 1450 °C (Figure 7, *a*). It was not possible to conduct X-ray examination at higher temperatures, as the molten slag melt starts bubbling at 1500 °C, that essentially distorts the slag melt free surface, the main requirements to which are absence of microroughnesses and horizontality. As the free surface of the liquid always tries to take a horizontal position, bubbling, similar to the boiling process, greatly distorts the surface.

As shown by electron microscopy investigations, the composition of the surface and bottom of crucible does not correspond to each other. So, fluorine content is much lower from the surface side (see Table 2), than from the bottom side of the crucible, i.e. from the bottom side the oxide component is smaller and the fluoride component is larger, making the molten flux in the point of contact with the metal even more acid.

In conclusion it should be noted that the conducted investigation showed the complex nature of interaction in the agglomerated flux before formation of the molten slag phase. Main structural changes at flux heating up to 1200 °C occur as a result of solid-phase interactions in the product, formed by liquid glass sintering with the adjacent main flux components. Formation of complex compounds of $AlCa_2Mg_5NaSi_7\times$ $\times O_{22}F_2$ type is possible.

In the temperature range of about 1200 °C formation of liquid phase by melting of the agglomerate of liquid glass with the main components and of complex unstable compounds begins. Here, anion redistribution between calcium and magnesium cations takes place. This results in formation of $CaAl_2Si_2O_8$ anorthite. Another product of decomposition of complex compounds can be formation of MgF_2 as a result of fluorine being in the immediate vicinity of magnesium in them. At 1350 °C, MgF_2 is the main crystalline phase against the background of the liquid phase.

At 1450 °C complete melting of the flux is observed, the melt, however, is not homogeneous, and the structures of the bottom and surface of the formed slag crust differ markedly.

The authors express their gratitude to Tokyo Boyoki Company and personally to V.A. Tinkov, Cand. of Phys.-Math. Sci., for conducting electron microscopy investigations and providing assistance in interpretation of the obtained data.

1. Podgaetsky, V.V., Kuzmenko, V.G. (1988) *Welding fluxes*. Kiev: Naukova Dumka.
2. Podgaetsky, V.V., Lyuborets, I.I. (1978) *Welding fluxes*. Kiev: Naukova Dumka.
3. Shpak, A.P., Sokolsky, V.E., Kazimirov, V.P. et al. (2003) *Structural peculiarities of melts of oxide systems*. Kiev: Akademperiodika.
4. Pashchenko, A.A., Myasnikov, A.A., Myasnikova, E.A. et al. (1986) *Physical chemistry of silicates*. Ed. by A.A. Pashchenko. Moscow: Vysshaya Shkola.
5. Berezhnoj, A.S. (1900) *Multicomponent oxide systems*. Kiev: Naukova Dumka.